Acústica 2020
XI Congreso Ibérico de Acústica
51º Congreso Español de Acústica
TECNIACÚSTICA 2020

ON THE NUMERICAL COMPUTATION OF TRANSMISSIBILITY OF VIBRATION, ACOUSTIC AND VIBRO-ACOUSTIC RESPONSES

Vasco M. N. Martins[1], Miguel M. Neves[2*]

[1] Instituto Superior Técnico, Universidade de Lisboa, Lisboa, Portugal
{vasco.mnmartins@gmail.com}
[2] IDMEC, Instituto Superior Técnico, Universidade de Lisboa, Lisboa, Portugal
{miguel.matos.neves@tecnico.ulisboa.pt}

Resumo
Nos últimos anos, observa-se um interesse crescente no uso do conceito de transmissibilidade para estimar respostas de vibração, respostas acústicas ou/e respostas vibroacústicas. Apesar do já conhecido potencial e das limitações nas suas aplicações, há uma necessidade considerável de pesquisa sobre as diferentes maneiras de executar o cálculo numérico da transmissibilidade. Neste texto, o autor revê e discute alguns aspectos da computação numérica da transmissibilidade.

Palavras-chave: transmissibilidade, vibração, acústica, vibroacústica, computação numérica.

Abstract
In recent years, it can be observed an increasing interest on the use of the transmissibility concept for estimation of vibration, acoustic or/and vibro-acoustic responses. Despite the known potential and limitation of its applications, there still be a considerable need for research on its different ways of performing the numerical computation of the transmissibility. In this text, the author review and discuss some aspects of the numerical computation of the transmissibility.

Keywords: transmissibility, vibration, acoustic, vibro-acoustic, numerical computation.

PACS no. 43.40.+s, 46.40.-f

1 Introduction

The dynamic transmissibility concept is well known in vibration and acoustic fields, but mainly in what concerns to a two degree-of-freedoms (DOFs) relation. Its generalization to a relation between multiple degrees-of-freedoms (MDOFs) – which are not necessarily aligned with one line– is more recent.
Initial attempts to achieve the mentioned generalization were found in Snowdon [1], Vakakis et al. [2] and Sciulli and Inman [3], Liu and Ewins [4], Varoto and McConnell [5], among others. First generalizations involving MDOFs are e.g. in [6-8], present a transmissibility matrix relating two sets of response positions.
In acoustics and vibro-acoustic fields this generalization to MDOFs relations – defining a multipoint transmissibility – is a more recent development with few publications available in the literature. Among them are the works of Curling and Païdoussis [9], Tcherniak and Schuhmacher [10], Devriendt et al. [11], Guedes [12], Guedes and Neves [13-14], Neves et al. [15], Martins [16] and Vaitkus et al. [17].

This transmissibility concept is of interest for many applications, in particular where one has technical difficulties in measuring the responses at some co-ordinates of the structure. It may be an alternative, when the transmissibility matrix of the original system can be evaluated or measured beforehand, case where it is to expect that in similar conditions one be able to estimate responses by measuring a few responses in accessible points, as described in Maia et al. [18].
It is well known that in the classical two-point vibration transmissibility case, the displacement and force transmissibility expressions are identical (in modulus). For MDOF relations, the force and displacement transmissibility expressions are not strictly identical, as mentioned in [19] and explained in [20].
In what concerns to published works in acoustic transmissibility, only a few are fully dedicated to it, while instead most of them appear in its applications e.g. in operational transfer path analysis (OTPA). Devriendt et al [21] applied a Finite Element based scalar pressure ratio transmissibility for an acoustic cavity. In the works Kletschkowski [22] and Weber et al [23] the authors perform identification of noise sources. Inspired on these works, Guedes and Neves [14] and Guedes [13] extended the concept to the 2D case for noise source identification and reconstruction. Experimental work performed to validate the method, can be find in [24].
The need for faster Transfer Path Analysis (TPA) methods [25] resulted in the development of Operational TPA (OTPA or OPA) methods [26]. But soon, several authors described limitations and drawbacks of these methods (see e.g. [27]) which includes difficulties related to the transmissibility's estimation, errors due to coupling between path, among others. In acoustic transmissibility applications, one can mention the works from Tcherniak [28] and Tcherniak and Schuhmacher [29].
In section 2, authors start with a brief revision of the fundamentals from vibration, acoustic as well as vibro-acoustic transmissibility concept (in the frequency domain). A brief verification of the acoustic transmissibility relation is presented at section 3. A brief verification of the vibro-acoustic transmissibility relation in an acoustic tube with an elastic plate at end is presented at section 4 including an analysis on the cross-talk problem. Finally, in section 5, authors elaborate on a verification test to perform with the OTPA and present first results of a work that is in progress at the moment.

2 Fundamentals

Concepts like vibration, acoustic and vibro-acoustic transmissibility between sets of DOFs are concisely reviewed in this section. For a more detailed description [12, 14, 17] are recommended.

2.1 Vibration transmissibility between sets of DOFs

For a linear viscoelastic solid, its structural response can be given by the following equilibrium equation

$$[M_s]\{\ddot{y}(t)\} + [C_s]\{\dot{y}(t)\} + [K_s]\{y(t)\} = \{f_s(t)\}, \tag{1}$$

where $[M_s]$, $[C_s]$, $[K_s]$ are the mass, damping and stiffness matrices of the solid 's', respectively; $\{y(t)\}$ is the nodal displacement vector; $\{f_s(t)\}$ is the excitation load vector and t is the time.
A steady-state response in case of harmonic excitation is obtained from

$$\left[[K_s] + \boldsymbol{i}\omega[C_s] - \omega^2[M_s]\right]\{Y(\omega)\} = \{F_s(\omega)\} \leftrightarrow [Z_s(\omega)]\{Y(\omega)\} = \{F_s(\omega)\}, \tag{2}$$

where $[Z_s(\omega)]$ is the dynamic stiffness matrix and ω the excitation frequency being applied. The response can be obtained using a receptance matrix $[H_s(\omega)]$ in the following form

$$\{Y(\omega)\} = [Z_s(\omega)]^{-1}\{F_s(\omega)\} = [H_s(\omega)]\,\{F_s(\omega)\}. \tag{3}$$

For the problem, it is usual to define some sets of DOFs. E.g., the K set composed of coordinates where the responses are measured, and the U set composed of coordinates where the displacements are unknown, while the A set of coordinates where loads are applied, (can therefore include part of U). The remaining set to be considered is the C one, which encompasses the remaining coordinates of the solid. Using the receptance matrix it is possible to relate the responses with the applied forces as

$$\{Y_U\} = [H_{s\,UA}]\{F_{s\,A}\}, \tag{4}$$

$$\{Y_K\} = [H_{s\,KA}]\{F_{s\,A}\}, \tag{5}$$

which allows to introduce a transmissibility matrix, that relate the measured responses with the unknown responses through the A set, as in the following relation

$$\{Y_U\} = [H_{s\,UA}]\,[H_{s\,KA}]^{+}\{Y_K\} = \left[\mathrm{T}_{\mathrm{UK}}^{\mathrm{A}\,(\mathrm{s})}\right]\{Y_K\}. \tag{6}$$

For the pseudo-inversion (+), one observe that in number of DOFs the set K needs to be greater than or equal to the dimension of the set A (i.e. in number of DOFs). If the sets have the same size, the pseudo-inversion turn into a regular inversion.

2.2 Acoustic pressure transmissibility between sets of DOFs

Much alike the vibrational case of the previous section, a linear acoustic fluid, with no flow, can be modelled, in a steady-state regime by

$$\left[[K_f] + \boldsymbol{i}\omega[C_f] - \omega^2[M_f]\right]\{P(\omega)\} = \{F_f(\omega)\} \leftrightarrow [Z_f(\omega)]\{P(\omega)\} = \{F_f(\omega)\}, \tag{7}$$

where $[M_f]$, $[C_f]$, $[K_f]$ are the mass, damping and stiffness matrices of the acoustic fluid '*f*', respectively; $\{P(\omega)\}$ is the nodal pressure vector; $\{F_f(\omega)\}$ is the excitation load vector and ω is the excitation frequency. The steady-state pressure $\{P(\omega)\}$ can therefore be obtained using a frequency response function (FRF) of the acoustic system $[H_f(\omega)]$

$$\{P(\omega)\} = [Z_f(\omega)]^{-1}\{F_f(\omega)\} = [H_f(\omega)]\,\{F_f(\omega)\}. \tag{8}$$

By taking into account that no other acoustic sources exist, besides the ones in set S, meaning that $\{F_{f\,K}\}$, $\{F_{f\,U}\}$, $\{F_{f\,C}\}$ are zero, one obtains:

$$\{P_K\ P_U\ P_S\ P_C\}^T = \left[H_{f\,KS}\ \ H_{f\,US}\ \ H_{f\,SS}\ \ H_{f\,CS}\right]^T \{F_{f\,S}\}. \tag{9}$$

which allows to relate $\{P_U\}$ with $\{P_K\}$ in the presence of a single source. The superscript 'T' means transpose. This relation comes in the form of acoustic pressure transmissibility $\left[\mathrm{T}_{\mathrm{UK}}^{\mathrm{S}\,(\mathrm{f})}\right]$

$$\{P_U\} = [H_{f\,US}]\,[H_{f\,KS}]^{+}\{Y_K\} = \left[\mathrm{T}_{\mathrm{UK}}^{\mathrm{S}\,(\mathrm{f})}\right]\{P_K\}. \tag{10}$$

2.3 Vibro-acoustic transmissibility between sets of DOFs

For the acoustic-structural coupled problem, the nodal pressure $\{P(\omega)\}$ from the acoustic medium manifests in the solid according to the following relation:

$$\left[[K_s] + \boldsymbol{i}\omega[C_s] - \omega^2[M_s]\right]\{Y(\omega)\} = \{F_s(\omega)\} - [A]\{P(\omega)\}\,, \tag{11}$$

with $[A]$ being the coupling matrix which transfer the pressure from the acoustic medium to the structure. A more detailed view of the topic can be found in [30, 31].
The fluid-structure interface (FSI) condition is given by:

$$\frac{\partial p}{\partial n} = -\rho\ddot{y}_n \tag{12}$$

conveys the displacement at the boundary into the acoustic fluid, i.e:

$$\left[\left[K_f\right] + \boldsymbol{i}\omega\left[C_f\right] - \omega^2\left[M_f\right]\right]\{P(\omega)\} = \left\{F_f(\omega)\right\} - \omega^2\,[A]^T\,\{Y(\omega)\}\,. \tag{13}$$

Combining the modified structural and acoustic finite elements (FE) from equations (11) and (13), one obtains

$$\left(\begin{bmatrix} K_s & A \\ 0 & K_f \end{bmatrix} + \mathbf{i}\omega\begin{bmatrix} C_s & 0 \\ 0 & C_f \end{bmatrix} - \omega^2\begin{bmatrix} M_s & 0 \\ -\rho A^T & M_f \end{bmatrix}\right)\begin{Bmatrix} \mathrm{Y}(\omega) \\ \mathrm{P}(\omega) \end{Bmatrix} = \begin{Bmatrix} F_s(\omega) \\ F_f(\omega) \end{Bmatrix}. \tag{14}$$

This Eulerian FE/FE coupled vibro-acoustic system [30] models a Fluid-Structure Interaction (FSI) and can ultimately be expressed as

$$([K^{FSI}] + \mathbf{i}\omega[C^{FSI}] - \omega^2[M^{FSI}])\{\mathrm{X}(\omega)\} = \{F^{FSI}\} \;\leftrightarrow\; \{\mathrm{X}(\omega)\} = [H^{FSI}]\{F^{FSI}\} \tag{15}$$

where $[M^{FSI}]$, $[C^{FSI}]$, $[K^{FSI}]$ are the mass, damping and stiffness matrices of the coupled vibro-acoustic problem, respectively; $\{P(\omega)\}$ is the nodal pressure vector; $\{Y(\omega)\}$ is the nodal displacement vector; $\{F^{FSI}\}$ is the excitation load vector and ω is the excitation frequency.
Now, if the same two regions from before are considered – K region, where the pressure responses are measured, and U region where the structural loads are applied (with consequent displacements of relevance) – one can write that

$$\{Y_U(\omega)\} = [H_{UU}^{FSI}]\{F_U(\omega)\}, \tag{16}$$

$$\{P_K(\omega)\} = [H_{KU}^{FSI}]\{F_U(\omega)\}. \tag{17}$$

The Figure 1 illustrates that this models involves a structure, an acoustic fluid and an interface between both. The vibro-acoustic transmissibility relating pressure with displacement responses is given by

$$\{P_K(\omega)\} = [H_{KU}^{FSI}][H_{UU}^{FSI}]^{-1}\{Y_U(\omega)\} = [T_{KU}^{FSI}]\{Y_U(\omega)\} \tag{18}$$

displayed as $[T_{KU}^{FSI}]$. This transmissibility matrix will have dimensions n_K x n_U , corresponding to the number of coordinates in both sets *K* and *U*.

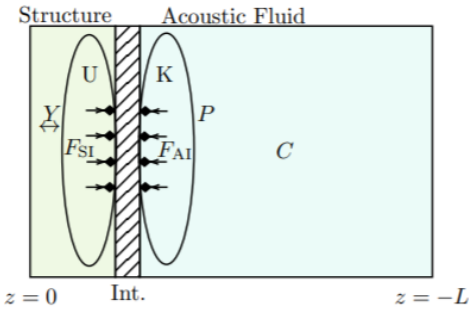

Figure 1 – Vibro-acoustic interaction depicted in sets of coordinates U, K and others C, for Y imposed excitation at structure and interface exaggerated to underline forces F_{SI} between structure and interface F_{SI} and F_{AI} between acoustic medium and interface.

3 On the contributions from acoustic transmissibility

It is known that in presence of several sources, the OTPA contributions (S'_n) for a response on a given point differ from the corresponding TPA ones (C_n) by a term related with the respective cross-talk effects, assumed of order ε^2 in some cases.

$$S'_1 + S'_2 = C'_1 + C'_2 + O(\varepsilon^2) \tag{19}$$

In order to verify the preposition that OTPA contributions differ from the TPA ones by the cross-talk effects, the following finite element model (Figure 2) was used.
It considers two acoustic sources u1 and u2 producing spherical waves, and twelve symmetrically disposed pressure sensors, v_A to v_F . A receiver y at middle of the tube is considered as the reference point to analyse the C_n contributions. An anechoic boundary is applied in all boundaries.
The dimensions for the box of the Figure 2, as well as the other properties, are presented in Table 1.

Table 1 – Box dimensions and fluid properties.

Property	Value
Length - L	4 m
Width and Height - b	2 m
Density - ρ	1.21 kg/m^3
Sound Speed - c	344 m/s

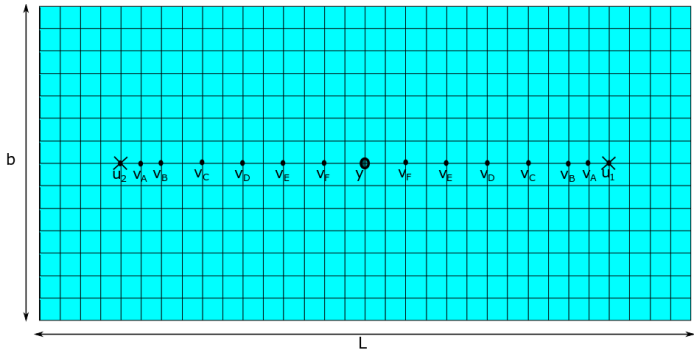

Figure 2 – Side view of the proposed 3D model (box dimensions: *Lxbxb*) with anechoic boundaries

From this model, the matrices $[M_f]$, $[C_f]$, $[K_{sf}]$ were computed, and from these $[Z_f(\omega)]$ is obtained and consecutively $[H_f(\omega)]$ using Eq. (7).

In this case, the spherical pressure waves being generated in a steady-state harmonic regime with an amplitude of 1 Pa, coming from the punctual sources u_1 and u_2. Then, the pressure values are measured directly from the twelve symmetric sensors v_i and the receiver y. The simulated wave pressure response is displayed in Figure 3.

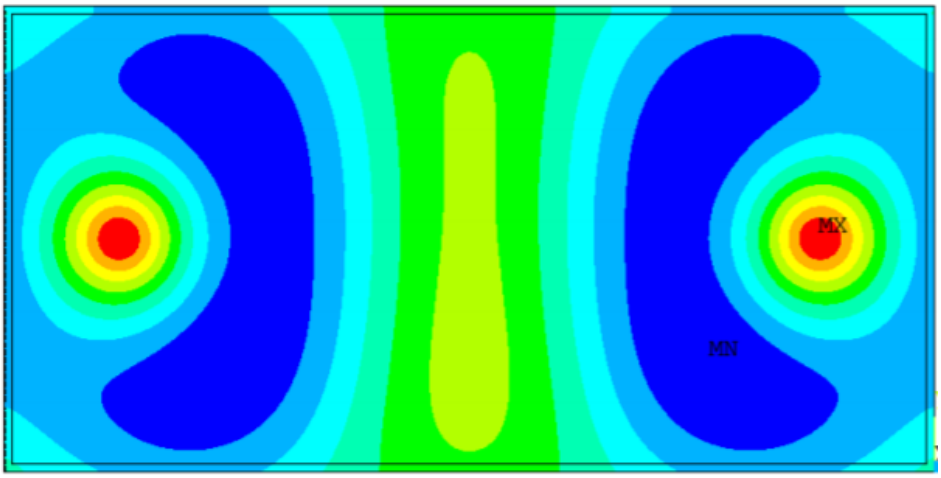

Figure 3 – Pressure response (50 Hz) for a highly refined mesh (in color: blue is the minimum value and red the maximum value)

Because it may be heavy to process computationally, a rule of tumble is to choose a refinement keeping in mind the frequency being analysed – in this analysis (50 Hz) – and that the number of elements per wavelength, longitudinally and transversely had to be at least 32. Here, 32 elements were considered longitudinally and 14 transversely.

The TPA contributions from the excitation sources C_n for the receiver Y position are:

$$Y = \sum_{n=1}^{N} C_n = \sum_{n=1}^{N} H_{nY} U_n. \tag{20}$$

The pressure at the receiver Y, can be estimated from the sensors V_i using the relation between the sensors and the sources, i.e. $\{V\} = [H_{UV}]\{U\}$, by

$$Y = [H_{YU}][H_{VU}]^{-1}\{V\}, \tag{21}$$

which essentially results in:

$$Y = \left\{ \frac{H_{YU_1}}{H^2_{V_1U_1}(1+\varepsilon)} \quad \frac{H_{YU_2}}{H^2_{V_1U_1}(1+\varepsilon)} \right\} \begin{Bmatrix} V_1 \\ V_2 \end{Bmatrix}. \tag{22}$$

where $\varepsilon = \frac{H_{V_1U_2}}{H_{V_1U_1}}$ is a cross talk measure from source 2 in the sensor 1.

Now, one can estimate the contribution S_n based on measures at sensor V_i positions i from A through F and compare with "true" contribution C_n. This was done with

$$C_n \approx S_n = T_{Yn} V_n. \tag{23}$$

On the other hand, without pondering the influence of ε, if the separate sensor contributions are added one can do the following estimative for each point of the sensors (*A,B, …, F*):

$$S_{(A\to F)} = T_{YV} V_{(A\to F)}. \tag{24}$$

The values obtained from equation (24) for Sn are presented in Table 2. The "true" contribution C_n is "measured" at x=2 m while the estimates S_n are computed with values obtained from each sensor V_i at respective position *i* from A through F (see lines 3 to 8 of Table 2). The cross-talk due to the second source – quantified at column of ε – affects the estimate S_n.

Table 2 – Contributions C_n and cross-talk levels ε at sensors v_i of Figure 2.

	Positions x(m)	C_n (Pa)	S_n (Pa)	ε	Sn-Cn (Pa)
y	-2	-0.0108	-	-	-
v_A	-0.625 and -3.375	-0.0108	-0.0107	0.0267	8.5713e-05
v_B	-0.75 and -3.25	-0.0108	-0.0103	0.0407	4.9923e-04
v_C	-1 and -3	-0.0108	-0.0098	0.1138	9.9933e-04
v_D	-1.25 and -2.75	-0.0108	-0.0142	0.2323	-0.0034
v_E	-1.5 and -2.5	-0.0108	-0.0164	0.4054	-0.0056
v_F	-1.75 and -2.25	-0.0108	-0.0233	0.6486	-0.0125
u_1	-0.5	-	-	-	-
u_2	-3.5	-	-	-	-

As expected, the level of cross-talk ε decreases with the reduction of the distance of the sensor V_i to the sources. Indeed, with a sensor near of the source the cross-talk is not enough to change significantly the estimate obtained with the transmissibility. In this case, the verification of the numerical calculus is achieved with success, although a more embracing study shall be performed for a better understanding of the use of the finite element model for these predictions.
In the Figure 4, is illustrated how the estimate S_1+S_2 differs from the value C_1+C_2 with the reduction of the distance of the sensor V_i to the sources. Small values of cross-talk like with sensors at v_A resulted in a cross-talk ε of 0.0267 (i.e. with a $\log_{10}\varepsilon$ =1.57). The difference between the estimate S_1+S_2 and the value C_1+C_2 is small in positions A, B and C, but for D, E and F is no more negligible as is evident from the S_n-C_n line.

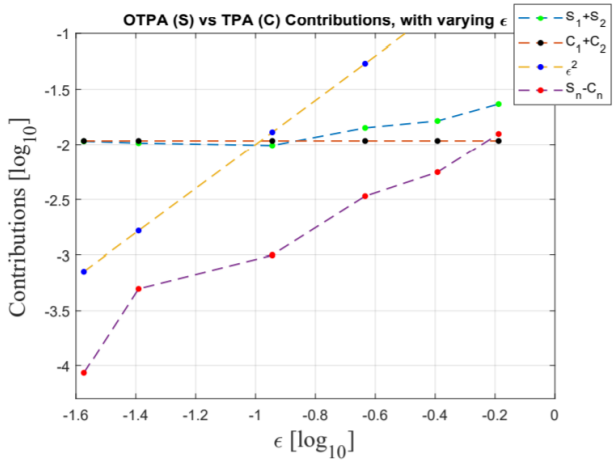

Figure 4 – Plot of C and S versus the cross-talk parameter ε (for a frequency of 50 Hz)

4 Verification of scalar vibro-acoustic transmissibility

In this section, the main purpose is to verify the numerical computations used to estimate the vibro-acoustic transmissibility with a finite element model. The verification consists in the comparison of the transmissibility results obtained via pressure/displacement ratio (using simulated measures of pressure and displacement) with the proposed frequency response matrix method indicated by (21).
For this verification, let us consider a long tube acoustic cavity coupled with a steel plate (by means of FSI), much like in [31]. This plate (in red at Figure 5) is located at the upstream end, from the center of the tube. A center-line is considered along the tube-plate system.
The tube-plate coupled system already meshed is represented in figure 5. The obtained natural frequencies of the system are indicated in the Table 5.

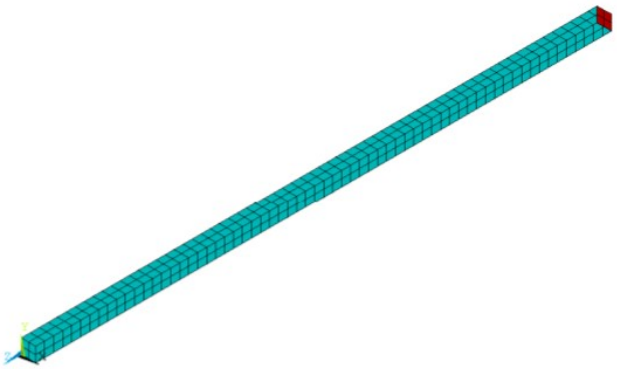

Figure 5 – Mesh for the tube- plate system with 64 tridimensional element divisions along the length, and with 4 elements in the transversal direction.

The properties for the tube and plate are presented in tables 3 and 4, respectively.

Table 3 – Acoustic Tube Properties.

Property	Value
Length - L	4 m
Width and Height - b Density - ρ	0.1 m 1.21 kg/m^3
Sound Speed – c	344 m/s
Reference Pressure - P_{ref}	1 Pa

Table 4 – Plate Properties.

Property	Value
Young's Modulus – E	210 GPa
Mass Density - ρ	7800 kg/m^3
Section Width and Height - b	0.1 m
Thickness – t	0.001 m
Poisson's Ratio - ν	0.3

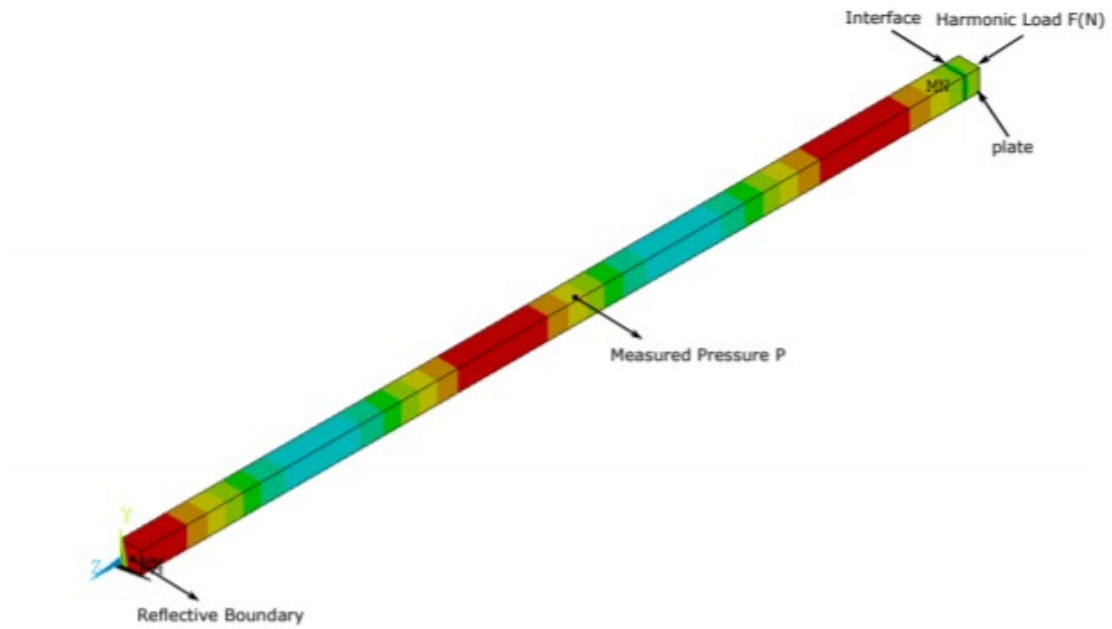

Figure 6 – Illustration of the pressure response (in color: blue is the minimum value and red the maximum value).

For this vibroacoustic model, the analysis follows what is described in section 2.3, where is a fluid-structure interface is applied between the upstream end of the acoustic tube and the end plate (Figure 6). First it is computed, from the finite element model, the ratio between the acoustic pressure measured in the center of the tube at the point P (subset *K*) and the dynamic displacement imposed at the center of the plate (subset *U*). After, for comparison it is computed the same transmissibility is obtained using the matrix method based in equation (18) i.e. by

$$\frac{H_{KU}^{FSI}}{H_{UU}^{FSI}} = \frac{H_{z=-L/2,z=-L}^{FSI}}{H_{z=-L,z=-L}^{FSI}}, \tag{25}$$

where both H_{KU} and H_{UU} are extracted from the original FR matrix $[H^{FSI}]$, accordingly, to the subsets of coordinates *K* and *U*. For comparison, the obtained results are in the Figure 7.

Table 5 – First thirteen natural frequencies (N.F.) of the coupled tube- plate system (without constraints) indicating the predominant mode type: A for acoustic and S for structural

N.F. *f*(Hz)	Mode type	N.F. *f*(Hz)	Mode type	N.F. *f*(Hz)	Mode type
0	A	216.08	A	390.46	A
45.530	A	259.39	A	434.61	A
87.363	A	302.87	A	479.02	A
130.01	A	346.56	A	-	-
172.95	A	354.32	S	-	-

From the observation of Figure 7, it is clear the almost coincidence of the two lines. As expected, the flat spots and peak transitions are situated on the resonance frequencies of the system. With these results, it is considered that the purpose of verifying the numerical computations done to estimate the vibro-acoustic transmissibility with a finite element model was achieved.

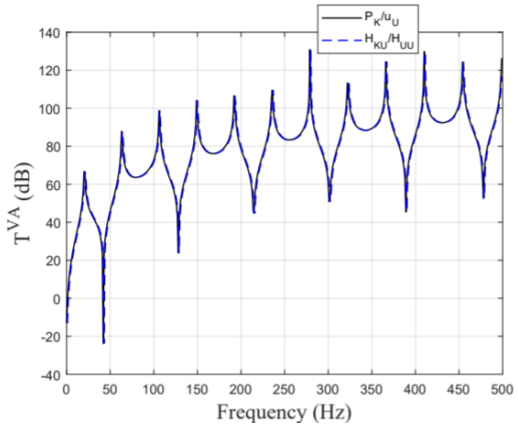

Figure 7 – Plot of the vibro-acoustic transmissibility between K and U obtained via pressure/displacement ratio and via frequency response matrix method (64 element divisions along the length, each division with 4 transverse elements).

5 Verification of the OTPA vibro-acoustic contributions

In this section, the purpose is to verify the finite element model in what concerns to obtain the OTPA contributions S' for the limit conditions of stiffness of the spring connections between the plate and the excitation vibration source. It is expected [15] to verify the following limit results.

$$\lim_{k1,k2\to 0} S_1' = C_1 \ , \lim_{k1,k2\to 0} S_2' = C_2 \ . \tag{26}$$

$$\lim_{k1,k2\to \infty} S_1' = S_1 \ , \lim_{k1,k2\to \infty} S_2' = S_2 \ . \tag{27}$$

For it, the vibro-acoustic coupled model presented in Figure 8 was devised. The mesh for this coupled FEM has 24 longitudinal elements (for the acoustic propagation) and 8 transverse elements. The upstream end (left end in Figure 8) of the acoustic box is anechoic.
The physical and geometric properties of the model in Figure 8 are the same given in Tables 1 and 4, with the exception that, in this case, the width *b* of the square plate is 2 m.
Two active (v_2 and v_4) and two passive (v_1 and v_3) sides are considered. The outer nodes of the plate are simply supported and the active nodes only move longitudinally. Two harmonic loads of 1 N are applied in these active nodes and the harmonic displacements are measured in all the accelerometers. From here, the OTPA contributions S' (to y) are estimated through vibro-acoustic transmissibility (with $T_i = H(v_i,y)/H(v_i,v_{2,4})$ and i = 1...4). These are then compared with the TPA ones, or the actual pressure value obtained from the receiver in y at middle of the tube.
Just as it was introduced in section 5, the purpose of the model in Figure 8 is the verification of OTPA expected response with mount (springs) stiffness k variation.
It can be stated from the values obtained that: if the stiffness of the mounts is considerably lower than the stiffness of corresponding plate node (for this example, ≈ 6 orders of magnitude), the OTPA (active) contributions are essentially the same of the baseline ones Cn (or y). For the rigid mount (≈ 6 orders of magnitude above plate stiffness), it is verified that the OTPA (active) contributions are in fact equal to the passive ones, in accordance with equation (27).

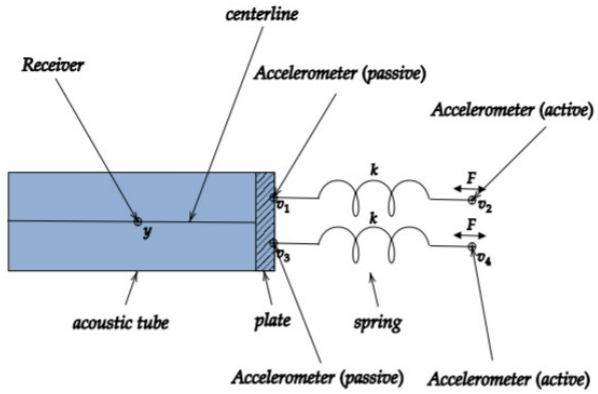

Figure 8 – System with two (spring) mounts on a steel plate coupled with an acoustic medium.

6 Conclusions

The intended verifications of the transmissibility concept (with the simple FE models developed) were successfully performed. Although it was not added noise in the "measured" signals at this step, the results are considered a starting point for a larger study on the understanding the potential and limitations of the use of vibro-acoustic transmissibility to estimated responses with cross-talk effects.

Acknowledgements

This work was supported by FCT, through IDMEC, under LAETA, project UIDB/50022/2020.

References

[1] Snowdon, J. C. Mechanical four-pole parameters: transmission matrices, *Report TM76-122*, Pennsylvania State University, Applied Research Lab, 1976. (https://apps.dtic.mil/dtic/tr/fulltext/u2/a034442.pdf)

[2] Vakakis, A.F.; Paipetis, S.A. The effect of a viscously damped dynamic absorber on a linear multi-degree-of-freedom system, *Journal of Sound and Vibration*, Vol. 105(1), 1986, pp. 49-60.

[3] Sciulli, D.; Inman, D. J. Comparison of single- and two-degree-of-freedom models for passive and active vibration isolation design, *SPIE 2720, Smart Structures and Materials*: Passive Damping and Isolation, 1996.

[4] Liu, W.; Ewins, D. J. Transmissibility Properties of MDOF Systems, *16th Intern Operational Modal Analysis Conf (IMAC XVI)*, Santa Barbara, California (USA), 1998, pp. 847-854.

[5] Varoto, P.S.; McConnell, K.G. Single Point vs Multi Point Acceleration Transmissibility Concepts in Vibration Testing, *12th Intern Modal Analysis Conf (IMAC XVI)*, Sta Barbara (USA), 1998, pp. 83-90.

[6] Maia, N.M.M.; Silva, J.M.M.; Ribeiro, A.M.R. Experimental Evaluation of the Transmissibility Matrix, *17th Intern. Modal Analysis Conf. (IMAC XVII),* Orlando, Florida (USA), 1999, pp.1126-1129.

[7] Ribeiro, A. M. R., Silva; J. M. M., Maia, N. M. M., On the Generalization of the Transmissibility Concept. *Mechanical Systems and Signal Processing*, Vol. 14(1), 2000, pp. 29-35.

[8] Maia, N. M. M.; Silva, J. M. M.; Ribeiro, A. M. R. The Transmissibility Concept in Multi-Degree-of-Freedom Systems, *Mechanical Systems and Signal Processing*, Vol. 1(15), 2001, pp. 129-137.

[9] Curlinf, L.L.R.; Païdoussis, M.P. A discrete method for the acoustic transmissibility of a pressure transducer-in-capsule arrangement, *Mechanical Systems and Signal Processing*, Vol. 9(3), 1995, pp. 225–41.

[10] Tcherniak, D.; Schuhmacher, A.P. Application of Transmissibility Matrix Method to NVH Source Contribution Analysis, *27th International Modal Analysis Conference (IMAC XXVII)*, Orlando (USA), 2009.

[11] Devriendt, C.; Presezniak, F.; Sitter, G. Operational acoustic modal analysis using transmissibility measurements, *ICSV 16*, edited by M. Pawelczyk and D. Bismor, 5-9 July, 2009, Krakow, Poland.

[12] Guedes, C. *Localização de fontes acústicas em interiores de avião usando o conceito de transmissibilidade*. Master's thesis (in Portuguese) , Instituto Superior Técnico, Universidade de Lisboa, 2016.

[13] Guedes, C.; Neves, M.M. A model-based acoustic source localization using the mdof transmissibility concept, *Euroregio 2016*, Porto, 2016.

[14] Neves, M.M.; Guedes, C. Multipoint transmissibility concept to estimate pressures at locations of difficult access, *Simpósio de Acústica e Vibrações*, IteCons, Coimbra, 2017.

[15] Neves, M.M; Policarpo, H.; Maia, N.M.M.; Tcherniak, D. A note on the use of vibro-acoustic transmissibility to estimate vibro-acoustic responses, *ICEDyn 2019,* Viana do Castelo, Portugal, 24–26 June 2019.

[16] Martins, V.M.N. *Vibration, Acoustic and Vibro-Acoustic responses using Transmissibility functions*. Master's thesis, Instituto Superior Técnico, Universidade de Lisboa, 2019.

[17] Vaitkus, D.; Tcherniak, D.; Brunskog, J. Application of vibro-acoustic operational transfer path analysis, *Applied Acoustics*, 154, 2019, pp. 201-212.

[18] Maia, N.M.M.; Almeida, R.A.A.; Urgueira, A.P.V. Understanding Transmissibility Properties, *26th Intern. Modal Analysis Conference (IMAC XXVI),* Orlando, Florida, USA, 2008.

[19] Maia, N.M.M.; Urgueira, A.P.V.; Almeida, R.A.B. Whys and Wherefores of Transmissibility , *Vibration Analysis and Control - New Trends and Developments, InTech*, 2011, pp. 187-216.

[20] Lage, Y.E.; Neves, M. M., Maia, N. M. M., Tcherniak, D., Force Transmissibility versus Displacement Transmissibility, *Journal of Sound and Vibration*, 333(22), 2014, pp. 5708-5722.

[21] Devriendt, C.; Presezniak, F.; Sitter, G. Operational acoustic modal analysis using transmissibility measurements, *ICSV 16*, edited by M. Pawelczyk and D. Bismor, 5-9 July, 2009, Krakow, Poland.

[22] Kletschkowski, T. *Inverse noise source identification in an aircraft cabin*. Univ of Applied Sciences, Hamburg, 2013.

[23] Weber, M.; Kletschkowski, T.; Sachau, D. Identification of noise sources by means of inverse finite element method using measured data. *Acoustics'08*, Paris, 2008.

[24] Neves, M.M.; Guedes, C. Multipoint transmissibility concept to estimate pressures at locations of difficult access, *Simpósio de Acústica e Vibrações*, IteCons, Coimbra, 2017.

[25] Van der Seijs, M., Klerk, D., Rixen, D., General framework for transfer path analysis: History, theory and classification of techniques, *Mechanical Systems and Signal Processing*, Vol. 68-69, 2016, pp. 217-244.

[26] De Sitter, G.; Devriendt, C.; Guillaume, P.; Pruyt, E. Operational transfer path analysis, *Mechanical Systems and Signal Processing*, Vol. 24(2), 2010, pp. 416–431.

[27] Gajdatsy, P.; Janssens, K.; Desmet, W.; Van der Auweraer, H., Application of the Transmissibility Concept in Transfer Path Analysis, *Mechanical Systems and Signal Processing*, Vol. 24(7), 2010, pp.1963-1976.

[28] Tcherniak, D. Application of operational noise path analysis to systems with rotational degrees of freedom, Sas, P., Bergen, B. (Eds.), *ISMA 2010,* Leuven, Belgium, (art. no. 528), 2010, pp. 3943-3952.

[29] Tcherniak, D.; Schuhmacher, A.P. Application of Transmissibility Matrix Method to NVH Source Contribution Analysis, *27th International Modal Analysis Conference (IMAC XXVII),* Orlando (USA), 2009.

[30] Desmet, W.; Vandepitte, D. Finite Element Method in Acoustics, *ISAAC 13 - International Seminar on Applied Acoustics*, Leuven, 2002.

[31] C. Howard, The University of Adelaide. Department of Mechanical Engineering. *Coupled Structural - Acoustic Analysis Using ANSYS*, Internal Report (2000) 1–15.